Nanoscale Res Lett (2009) 4:1059–1063
DOI 10.1007/s11671-009-9357-z

NANO EXPRESS

Anodic Aluminum Oxide Membrane-Assisted Fabrication of β-In_2S_3 Nanowires

Jen-Bin Shi · Chih-Jung Chen · Ya-Ting Lin · Wen-Chia Hsu · Yu-Cheng Chen · Po-Feng Wu

Received: 9 March 2009 / Accepted: 24 May 2009 / Published online: 6 June 2009

Abstract In this study, β-In_2S_3 nanowires were first synthesized by sulfurizing the pure Indium (In) nanowires in an AAO membrane. As FE-SEM results, β-In_2S_3 nanowires are highly ordered, arranged tightly corresponding to the high porosity of the AAO membrane used. The diameter of the β-In_2S_3 nanowires is about 60 nm with the length of about 6–8 μm. Moreover, the aspect ratio of β-In_2S_3 nanowires is up to 117. An EDS analysis revealed the β-In_2S_3 nanowires with an atomic ratio of nearly S/In = 1.5. X-ray diffraction and corresponding selected area electron diffraction patterns demonstrated that the β-In_2S_3 nanowire is tetragonal polycrystalline. The direct band gap energy (E_g) is 2.40 eV from the optical measurement, and it is reasonable with literature.

Keywords Nanomaterials · In_2S_3 · Nanowire · AAO

Introduction

Nowadays, one-dimensional (1-D) nanomaterials (nanorods, nanowires, nanobelts and nanotubes) have been attractive due to their physical and chemical properties. These nanostructures in particular show results in electronics [1], magnetic [2], optics, etc., that have great potential applications in the next generation of nanodevices [3]. Various methods such as chemical vapor deposition (CVD), laser ablation, thermal evaporation, hydrothermal process, and anodic aluminum oxide (AAO) membrane-assisted synthesis method have been employed to prepare 1-D nanomaterials. AAO membrane-based assembling has been widely applied in recent years to produce nanowires with extremely long length and high aspect ratios, and it also provides a simple, rapid and cheap way for fabricating nanowires as aligned arrays [4, 5].

Indium sulphide (In_2S_3) is an III-VI compound material, and it exists in three phases at normal pressure: α (cubic), β (tetragonal) and γ (trigonal) [6]. β-In_2S_3, an ordered-defect superstructure of the defect-spinel α-In_2S_3, is stable below 420 °C [6], whereas γ-In_2S_3 is only stable above 754 °C, unless by adding As or Sb [7]. β-In_2S_3 crystal is known an n-type semiconductor with the band gap energy of 2.0 eV [6]. Furthermore, its photoconductive properties make it a promising candidate for photovoltaic applications such as solar cells [8]. Solar cell devices prepared by using β-In_2S_3 as a buffer layer show 16.4% conversion efficiency, which is very close to that of the standard CdS buffer layer [9].

A variety of methods have been developed into synthesized In_2S_3 powder, thin films, and nanofibers. Powder of β-In_2S_3 was synthesized using indium chloride ($InCl_3$) and thioacetamide (CH_3CSNH_2) as precursors via the sonochemical route [10]. β-In_2S_3 thin films were prepared using the CSP technique, and the spray solutions were mixtures of indium chloride ($InCl_3$) and thiourea ($CS(NH_2)_2$) [11]. In addition, β-In_2S_3 nanofibers were prepared using indium chloride and thiourea as source precursors by hydrothermal method with AAO membrane at 150 °C for 15 h. [12]. However, β-In_2S_3 nanowires were fabricated within AAO template synthesis, using the electrodeposition and sulfurizing methods that are not yet reported.

J.-B. Shi · W.-C. Hsu
Department of Electronic Engineering, Feng Chia University, Taichung 40724, Taiwan

C.-J. Chen · Y.-T. Lin (✉) · Y.-C. Chen · P.-F. Wu
The Graduate Institute of Electrical and Communications Engineering, Feng Chia University, 100, Wen-Hwa Rd, Seatwen, Taichung 40724, Taiwan
e-mail: p9431597@fcu.edu.tw

To fabricate the β-In_2S_3 nanowires, an effective and economical technique-anodic alumina oxide (AAO) membrane-assisted method was utilized in this study. The microstructure and optical properties of β-In_2S_3 nanowires are discussed.

Experimental

Porous anodic aluminum oxide (AAO) membrane with average channel diameter of 60 nm and thickness of 25 μm was fabricated by two-step anodization process as described previously [4, 5]. First, high purity aluminum sheet (99.9995%) was anodized in the oxalic acid solution under constant voltage 40 V for several hours. Subsequently, the anodized Al sheet was put into H_3PO_4 solution to completely remove the alumina layer. The AAO membrane can be fabricated by repeating the anodization process under the same conditions of the first step anodization. After the anodization, the AAO membrane was obtained by etching away the underlying aluminum substrates with $HgCl_2$ solution. The transparent AAO membrane was immersed in H_3PO_4 solution to widen the nanochannels. Finally, the diameter of the nanochannel was about 60 nm.

In order to prepare for pure Indium (In) nanowires, a layer of Pt was sputtered onto one side of the membrane acting as the working electrode in a standard two-electrode electrochemical cell. Pure Indium (In) was electrodeposited inside the nanochannels of the AAO membrane under constant voltage, using an electrolyte containing $In(SO_4)_3$, H_3BO_3, and distilled water. The AAO membrane with pure Indium (In) nanowires was washed with distilled water and air dried, put into a glass tube and together with sulfur powder (99.99%). The glass tube was evacuated by using a pump, and it was placed into the furnace. The samples were then heated from room temperature (heating rate: 5 °C/min) to 500 °C and held at this temperature for 10 h to completely sulfurize the pure Indium (In) nanowires. It is expected that S atoms would react with the In to form β-In_2S_3.

The morphologies of the as-prepared AAO membrane and the β-In_2S_3 nanowires were analyzed by field emission scanning electron microscopy/energy dispersive spectrometer (FE-SEM/EDS, HITACHI S-4800). The crystal structure of the nanowires was examined by X-ray diffraction (XRD, SHIMADZU XRD-6000) utilizing Cu Kα radiation. More details about the microstructure of the β-In_2S_3 nanowires were investigated by the high-resolution transmission electron microscopy/corresponding selected area electron diffraction (HR-TEM/SAED, JEOL JEM-2010). For HR-TEM and SAED analysis, the β-In_2S_3 nanowires were dispersed in ethanol and vibrated for few minutes. Then, a few drops of the resulting suspension were dripped onto a copper grid. For optical analysis, the AAO membrane was dissolved by NaOH solution at room temperature and washed with distilled water to expose freely nanowires of β-In_2S_3. After the β-In_2S_3 nanowires are absolutely dispersed in distilled water using a supersonic disperser, the absorption spectra of the β-In_2S_3 nanowires were measured on an UV/Visible/NIR spectrophotometer (HITACHI U-3501).

Results and Discussion

According to the FE-SEM images of Fig. 1a, it can be seen the surface of AAO membrane was still kept clean after pure Indium (In) nanowires were sulfurized at 500 °C for 10 h. Figure 1b shows a typical FE-SEM image for the cross-section image of β-In_2S_3 nanowires. It can be clearly seen that the β-In_2S_3 nanowires were wellfilled in nanochannels of the AAO membrane. The length of the β-In_2S_3 nanowires was in the average range 6–8 μm with the aspect ratio around 117. Figure 1c reveals the high-magnification FE-SEM image, it can be observed that the β-In_2S_3 nanowires were independent and parallel to each other with the diameter, which is about 60 nm. The EDS spectrum of the β-In_2S_3 nanowires is not shown. The result of EDS measurement reveals the atomic ratio of In and S with 41.79:58.21 and is very close to 1:1.5, which is in good agreement with the XRD result. After dissolving the AAO membrane by thorough chemical etching and followed by rinsing with distilled water, the β-In_2S_3 nanowires are still on the conducting substrate surface (Pt). Figure 1d reveals the β-In_2S_3 nanowires without AAO membrane. When the AAO membrane was dissolved away, the individual β-In_2S_3 nanowires were observed almost the same with the diameter of the channels of the AAO membrane. Thus, it can be seen the dimension of the β-In_2S_3 nanowires was controlled by AAO membrane.

Figure 2 shows the X-ray powder diffraction (XRD) spectra of the as-prepared β-In_2S_3 nanowires without AAO membrane, which makes the crystal structure of the β-In_2S_3 nanowires convenient for characterization. All the peaks were indexed as the reported data for β-In_2S_3 (JCPDS Card no. 32-0456). After the pure Indium (In) nanowires were completely sulfurized, no diffraction peaks of In and S or other impurities have been found. Furthermore, the In peaks totally disappear and the β-In_2S_3 peaks appear after sulfurize the pure Indium (In) nanowires. Metal oxides such as In_2O_3 nanowires have been prepared by oxidation of pure Indium (In) nanowires [13], and it is generally accepted that the chemical reaction of oxidation and sulfurization are similar to each other. Hence, the technique used here for formation of β-In_2S_3 is understandable. The reaction equation of β-In_2S_3 nanowires can be expressed as follows:

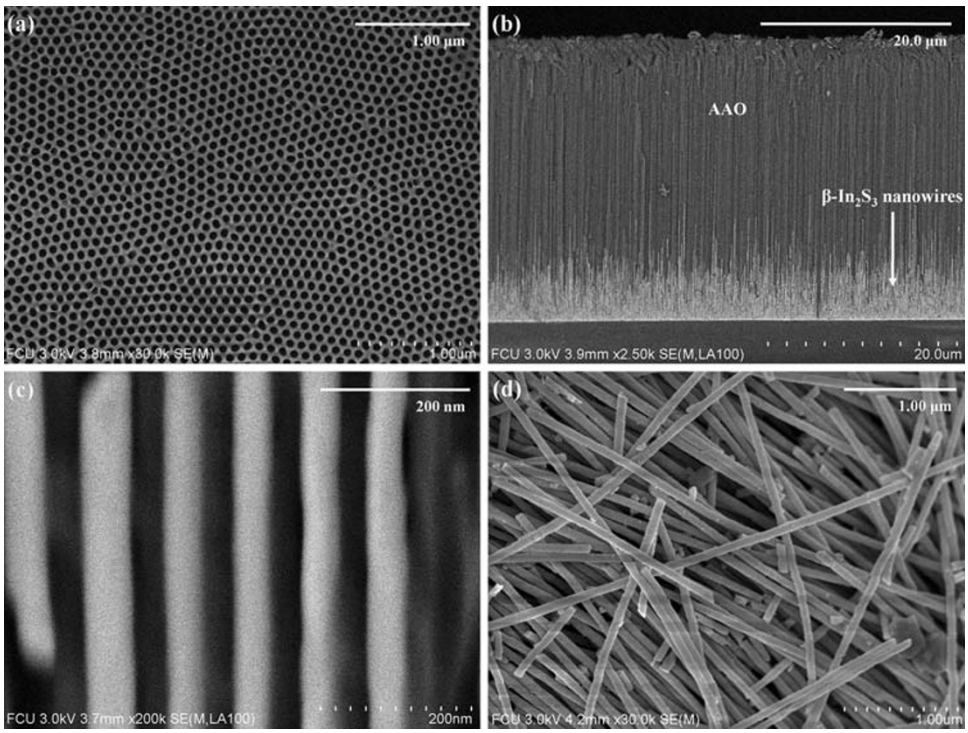

Fig. 1 FE-SEM images of **a** plane-view, **b** cross-section view of β-In_2S_3 nanowires arrays with the pore diameter of about 60 nm in the AAO membrane, **c** cross-section view at high magnification of β-In_2S_3 nanowires arrays in the AAO membrane, and **d** the AAO membrane was absolutely dissolved in NaOH solution

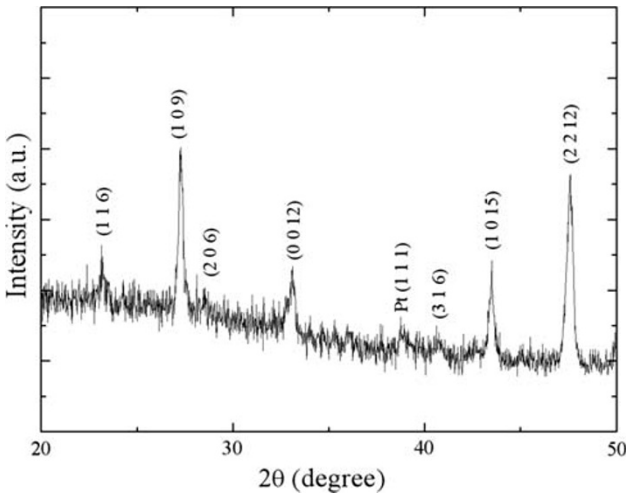

Fig. 2 X-ray diffraction patterns of β-In_2S_3 nanowires without AAO membrane

$$In + S \rightarrow In_2S_3 \quad (1)$$

In which the S atoms would react with In atoms at high temperatures to form β-In_2S_3 nanowires. The completeness of reaction is mainly dominated by time and temperature, long periods and high temperatures of the sulfurization process were needed to prepare the fine crystalline β-In_2S_3 nanowires. We observed that the β-In_2S_3 nanowires were completely formed when the sulfurization time reached to 10 h and the temperatures up to 500 °C.

Detailed information on the microstructure of as-prepared β-In_2S_3 nanowires was obtained by HR-TEM. Low-magnification HR-TEM image (Fig. 3a) illustrates the numerous β-In_2S_3 nanowires. Figure 3b reveals the HR-TEM image of an individual β-In_2S_3 nanowire. The diameter of the nanowire is about 60 nm. In Fig. 3c, the corresponding SAED pattern of an individual nanowire exhibits a polycrystalline. Moreover, the concentric diffraction rings could be indexed outwards as (2 2 12), (1 0 9), (0 0 12) and (1 0 3) lattice planes of tetragonal β-In_2S_3. The HR-TEM image of the nanowires (Fig. 3d) shows the parallel fringes with a spacing of 0.1913 nm, which can be assigned to the (2 2 12) plane of β-In_2S_3.

Figure 4 shows the UV/Visible/NIR absorption spectra of the as-grown β-In_2S_3 nanowires, recorded in the wavelength range 200–900 nm, which obviously reveals a broad absorption peak around 350 nm. Recently, Shen et al. reported that the bulk of In_2S_3 was prepared by $In(NO_3)_3 \cdot 4.5H_2O$ with H_2S at 300 °C for 3 h in the muffle oven [14]. They observed an absorption onset of bulk In_2S_3 at 650 nm. In addition, In_2S_3 colloidal thin films were synthesized by the spin-coating method [15]. They prepared a yellow colloid suspension by adding H_2S gas into an $InCl_3$ solution, containing a small amount of acetic acid as a stabilizer. The thin film was heated at 400 °C for 30 min under a N_2 atmosphere. In_2S_3 colloidal thin films have an absorption edge at about 550 nm. Furthermore, flowerlike β-In_2S_3 assembled with nanoflakes were synthesized by the hydrothermal method using $InCl_3 \cdot 4H_2O$ and L-cysteine [16].

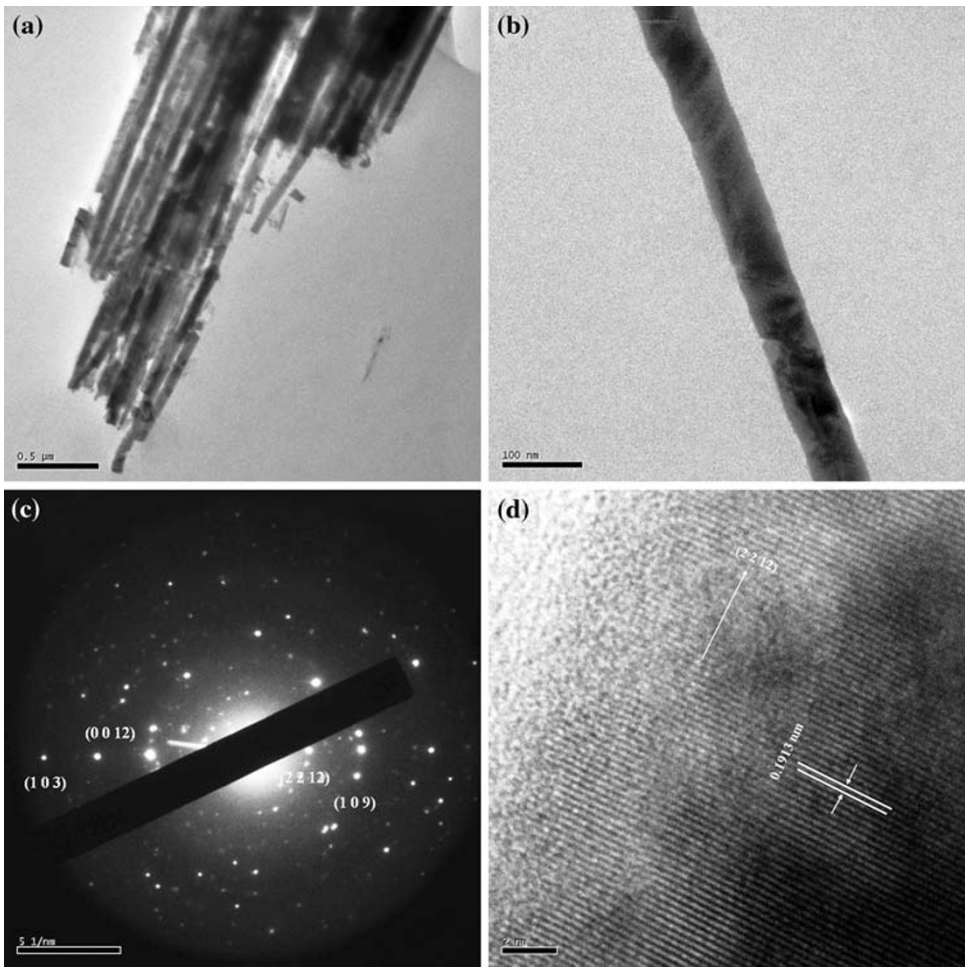

Fig. 3 **a** The low-magnification HR-TEM image of β-In_2S_3 nanowires, **b** the high-magnification HR-TEM image of an individual β-In_2S_3 nanowire, **c** SAED pattern of an individual β-In_2S_3 nanowire, and **d** HR-TEM image of a single β-In_2S_3 nanowire with lattice fringes

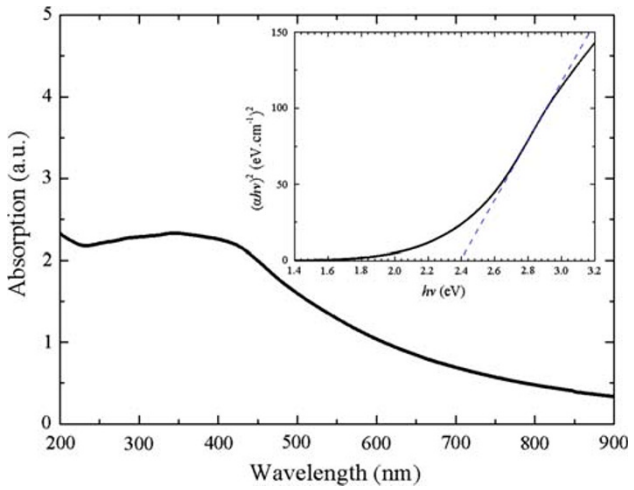

Fig. 4 UV/Visible/NIR absorption spectra with β-In_2S_3 nanowires and $(\alpha hv)^2$ versus hv plot (*inset*)

The absorption peak of In_2S_3 flowerlike is located at 395 nm. In addition, In_2S_3 hollow spheres were prepared by dodecanethiol-assisted hydrothermal process at 180 °C for 12 h, employing $InCl_3{\cdot}4H_2O$ and L-cysteine as precursors [17]. They observed an absorption peak of In_2S_3 hollow spheres located at 251 nm. However, our value of absorption peak is between the largest value of bulk (650 nm) and the smallest value of hollow spheres (251 nm). Our value of absorption peak is reasonable with literature [14–17].

In order to determine the band gap energy (E_g) of the β-In_2S_3 nanowires, the optical absorption coefficient (α) at the absorption edge may be expressed as [18]:

$$\alpha hv = A(hv - E_g)^m \quad (2)$$

where hv is the photon energy, A is the optical transition dependent constant, E_g is the optical band gap, and m is a constant that depends on the types of transitions involved. The values of $m = 1/2$, 3/2, 2, and 3 are for direct allowed, direct forbidden, indirect allowed, and indirect forbidden transitions, respectively. This equation gives band gap (E_g), when straight portion of $(\alpha hv)^{1/m}$ against hv plot is extrapolated to the point $\alpha = 0$. The analysis of the absorption spectra obtained for our samples shows that the spectral variation of the absorption coefficient, within the fundamental absorption region can be fitted by Eq. 2.

However, $m = 3/2$, 2, and 3, the band gap energies were found to be a negative number, which is not reasonable in physics. The inset in Fig. 4 shows the $(\alpha hv)^2$ against hv plot. Relationship fitting to the absorption spectra of β-In_2S_3 as $m = 1/2$, which is the allowed direct transition for these nanowires. In this inset figure, we observed that the curve has a very good straight line fit from 2.7 to 2.9 eV. This result indicates that the optical energy gap is direct transition. We also observed that the curve has been breakaway this line range when the photon energy is above 2.9 eV. The band gap energy (E_g) of β-In_2S_3 nanowires with diameter of about 60 nm is estimated to be 2.40 eV as $m = 1/2$ for extrapolation. In literature [19], powder of β-In_2S_3 was synthesized using $InCl_3$ and CH_3CSNH_2 as precursors followed by annealing in Ar atmosphere in the temperature range 573–1,123 K. The grain size of powder varied in the range 0.40–1.48 μm for different annealing temperatures. The band gap energy of β-In_2S_3 powder for various grain sizes was between 2.12 and 2.14 eV. Moreover, thin films of In_2S_3 were prepared from In_2S_3 powder using vacuum evaporation with resistively heated graphite crucible [20]. The average grain sizes of In_2S_3 thin film were around 0.22 μm. The optical band gaps of In_2S_3 thin film for different annealing temperatures and times were between 1.75 and 2.19 eV. β-In_2S_3 films were prepared by rapid heating of metallic Indium (In) films in H_2S atmosphere [21]. The grain sizes of the β-In_2S_3 films were in the range 22–30 nm. The films exhibit the higher band gap of 2.58 eV. Consequently, our band gap energy of β-In_2S_3 nanowires with 60 nm is between the largest band gap energy with grain sizes of 22–30 nm (2.58 eV) and the smallest band gap energy with grain sizes around 0.22 μm (1.75 eV). Our band gap energy of β-In_2S_3 nanowires with 60 nm is acceptable with literature [19–21].

Conclusions

In summary, we have presented a simple, inexpensive, and reasonable method to fabricate β-In_2S_3 nanowires. The β-In_2S_3 nanowires were first fabricated by sulfurizing the pure Indium (In) nanowires at 500 °C for 10 h, which is embedded in an AAO membrane. β-In_2S_3 nanowires have high wire packing densities with uniform wire diameters and lengths of about 60 nm and 6–8 μm, respectively. The analysis of the HR-TEM/SAED revealed that the β-In_2S_3 nanowire is polycrystalline. The β-In_2S_3 nanowires exhibited a linear relationship at 2.7–2.9 eV as $m = 1/2$, indicating that the direct band gap energy is 2.40 eV.

Acknowledgments The research was supported by the National Science Council of R.O·C. under grant No. NSC-96-2122-M-035-003-MY2.

References

1. G. Yi, W. Schwarzacher, Appl. Phys. Lett. **74**, 1746 (1999). doi:10.1063/1.123675
2. C.A. Ross, M. Hwang, M. Shima, H.I. Smith, M. Farhoud, T.A. Savas et al., J. Magn. Magn. Mater. **249**, 200 (2002). doi:10.1016/S0304-8853(02)00531-0
3. M.P. Zach, K.H. Ng, R.M. Penner, Science **290**, 2120 (2000). doi:10.1126/science.290.5499.2120
4. J.B. Shi, Y.J. Chen, Y.T. Lin, C. Wu, C.J. Chen, J.Y. Lin, Jpn. J. Appl. Phys. **45**, 9075 (2006). doi:10.1143/JJAP.45.9075
5. J.B. Shi, Y.C. Chen, C.W. Lee, Y.T. Lin, C. Wu, C.J. Chen, Mater. Lett. **62**, 15 (2008). doi:10.1016/j.matlet.2007.04.060
6. R. Diehl, R. Nitsche, J. Cryst. Growth **28**, 306 (1975). doi:10.1016/0022-0248(75)90067-6
7. R. Diehl, C.D. Carpentier, R. Nitsche, Acta Crystallogr. B **32**, 1257 (1976). doi:10.1107/S0567740876005062
8. R.H. Bube, W.H. McCaroll, J. Phys. Chem. Solids **10**, 333 (1959). doi:10.1016/0022-3697(59)90010-1
9. N. Barreau, S. Marsillac, D. Albertini, J.C. Bernede, Thin Solid Films **403–404**, 331 (2002). doi:10.1016/S0040-6090(01)01512-7
10. S. Gorai, S. Chaudhuri, Mater. Chem. Phys. **89**, 332 (2005). doi:10.1016/j.matchemphys.2004.09.009
11. T.T. John, C.S. Kartha, K.P. Vijayakumar, T. Abe, Y. Kashiwaba, Vacuum **80**, 870 (2006). doi:10.1016/j.vacuum.2005.11.046
12. X. Zhu, J. Ma, Y. Wang, J. Tao, J. Zhou, Z. Zhao, L. Xie, H. Tian, Mater. Res. Bull. **41**, 1584 (2006). doi:10.1016/j.materresbull.2005.12.016
13. M.J. Zheng, L.D. Zhang, G.H. Li, X.Y. Zhang, X.F. Wang, Appl. Phys. Lett. **79**, 839 (2001). doi:10.1063/1.1389071
14. S. Shen, L. Guo, J. Solid State Chem. **179**, 2629 (2006). doi:10.1016/j.jssc.2006.05.010
15. Y. Yasaki, N. Sonoyama, T. Sakata, J. Electroanal. Chem. **469**, 116 (1999). doi:10.1016/S0022-0728(99)00184-9
16. L.Y. Chen, Z.D. Zhang, W.Z. Wang, J. Phys. Chem. C **112**, 4117 (2008). doi:10.1021/jp710074h
17. P. Zhao, T. Huang, K. Huang, J. Phys. Chem. C **111**, 12890 (2007). doi:10.1021/jp073390l
18. G. Burns, *Solid State Physics* (Academic Press, Orlando, 1985)
19. S. Gorai, P. Guha, D. Ganguli, S. Chaudhuri, Mater. Chem. Phys. **82**, 974 (2003). doi:10.1016/j.matchemphys.2003.08.013
20. A. Timoumi, H. Bouzouita, R. Brini, M. Kanzari, B. Rezig, Appl. Surf. Sci. **253**, 306 (2006). doi:10.1016/j.apsusc.2006.06.003
21. R. Yoosuf, M.K. Jayaraj, Sol. Energy Mater. Sol. Cells **89**, 85 (2005). doi:10.1016/j.solmat.2005.01.004